crystals

MDPI

Article

Nb-Doped $0.8BaTiO_3$-$0.2Bi(Mg_{0.5}Ti_{0.5})O_3$ Ceramics with Stable Dielectric Properties at High Temperature

Feng Si, Bin Tang *, Zixuan Fang and Shuren Zhang

State Key Laboratory of Electronic Thin Films and Integrated Devices,
University of Electronic Science and Technology of China, Chengdu 610054, China;
sifeng928@163.com (F.S.); ZXFANG2015@163.com (Z.F.); zsr@uestc.edu.cn (S.Z.)
* Correspondence: tangbin@uestc.edu.cn

Academic Editor: Haidong Zhou
Received: 6 April 2017; Accepted: 3 June 2017; Published: 11 June 2017

Abstract: Nb-doped $0.8BaTiO_3$-$0.2Bi(Mg_{0.5}Ti_{0.5})O_3$ ceramics were prepared by conventional solid-state method. The dielectric properties and the structural properties were investigated. When Nb_2O_5 is doped into 0.8BT-0.2BMT system, a small amount of $Ba_4Ti_{12}O_{27}$ secondary phase is formed. The lattice parameters gradually increase with the Nb_2O_5 doping. It is found that the temperature-capacitance characteristics greatly depend on Nb_2O_5 content. With the addition of 3.0 mol% Nb_2O_5, a 0.8BT-0.2BMT ceramic sample could satisfy the EIA X9R specification. This material is promising for high-temperature MLCC application.

Keywords: barium titanate; X9R; dielectric ceramics; MLCC

1. Introduction

Multilayer ceramic capacitors (MLCC) have been extensively used in many kinds of electronic products in the last few decades. Some harsh conditions—such as downhole drilling, aerospace, and automotive environment—require the capability of MLCCs to withstand temperatures over 200 °C or more [1,2]. By contrast, the X7R (−55 to 125 °C, $\Delta C/C_{25\,^\circ C} \leq 15\%$) and the X8R (−55 to 150 °C, $\Delta C/C_{25\,^\circ C} \leq 15\%$)-type MLCCs defined by the Electronic Industries Association (EIA) standards are not competent because their ceiling temperatures are 125 °C and 150 °C, respectively [3,4]. Therefore, it is of great significance to exploit a material used for X9R (−55 to 200 °C, $\Delta C/C_{25\,^\circ C} \leq 15\%$)-type MLCCs, and develop a new temperature-stable dielectric material with high-temperature resistance, high dielectric constant, and low dielectric loss.

As well known, high permittivity MLCCs are generally derived from perovskite structures, such as barium titanate (BT) dielectric ceramics. As the Curie temperature (T_c) of BT is approximately 130 °C, however, it is difficult to prepare pure $BaTiO_3$ (BT) ceramics with weak temperature dependence [5]. Recently, $Bi(Me)O_3$ based perovskite (Me = Sc, Al, $Zn_{1/2}Ti_{1/2}$, etc.) were of interest for the study and development of new dielectric ceramics because of their relatively high dielectric constant, broad diffused dielectric behavior, and high Curie temperature [6–9]. Therefore, perovskite solid solutions based on BT-$Bi(Me)O_3$ composition with a high permittivity are developed and explored for high temperature capacitor applications [10]. The 0.8BT-0.2BMT ceramic with moderate dielectric constant and dielectric loss is reported to possess lower temperature variation of capacitance in high temperature regions [11]. The Nb_2O_5 doped BT systems are reported for potential application in advanced X8R capacitors, but the Nb_2O_5 dopant depressed dielectric constant in exchange for temperature stability [12]. The Nb^{5+} ion was found to diffuse into the crystal lattice and form the chemically inhomogenous regions, called 'core-shell' structure, showing good dielectric stability [13–15]. In this study, the 0.8BT-0.2BMT dielectric system is modified only by Nb_2O_5 to improve the dielectric temperature stability.

2. Experimental Procedure

Nb-doped 0.8$BaTiO_3$-0.2$Bi(Mg_{0.5}Ti_{0.5})O_3$(0.8BT-0.2BMT) ceramics were prepared using solid-state reaction method. $BaTiO_3$ (99.9%), Bi_2O_3 (99.0%), MgO (99%), and TiO_2 (99.0%) powders and Nb_2O_5 (99.5%) with different doped levels ($0 \leq x \leq 3$ mol%) were batched stoichiometrically and ball milled in a polyethylene jar with yttria-stabilized zirconia balls and de-ionized water for 4 h at a rate of 280 rpm. Then the mixtures were dried and calcined in alumina crucibles at 900 °C for 2 h. Subsequently, the calcined powders were then re-milled in de-ionized water using zirconia balls for 4 h. After drying, the resulting powders were granulated with a few drops of PVA binder and pressed into disk with 12 mm in diameter and 1 mm in thickness. Samples were sintered at 1120 °C for 2 h in air with a heating rate of 3 °C/min and then cooling with furnace to ambient temperature.

Crystal structure of the samples was determined at room temperature by X-ray powder diffraction (XRD) (Cu Kα radiation, PANalytical X'Pert Pro, Almelo, The Netherlands). Rietveld refinement of the crystal structures was performed using the GSAS-EXPGUI program [16]. Microstructure and composition analysis of the ceramic pellets were performed by scanning electron microscopy (SEM, Inspect F, FEI Company, Eindhoven, The Netherlands), which was operated at 20 kV. After samples were fired at 800 °C with silver paste on both sides, the room temperature dielectric constant and dielectric loss were measured by use of a precision LCR meter (4284A, Aglient) at 1 kHz and 1 Vrms. The temperature-capacitance characteristics of the samples were measured from –55 °C to 200 °C with LCR meter (4284A, Aglient) and an automatic temperature controller at 1 kHz and 1 Vrms with a rate of 2 °C/min. The insulation resistance of the specimens was recorded by a Digital Super Megohm Meters (DSM-8104, HIOKI, Nagano, Japan) at 25 °C. The bulk density was measured using the Archimedes method.

3. Results and Discussion

Figure 1 shows the XRD patterns of well-sintered Nb_2O_5 doped 0.8BT-0.2BMTceramic disks. All the samples presented a desired perovskite structure and no secondary phase was discovered for sample without Nb_2O_5 dopants. It indicated that homogeneous solid solution of 0.8BT-0.2BMT was obtained. However, a small amount of secondary phase $Ba_4Ti_{12}O_{27}$ is found in all Nb-doped 0.8BT-0.2BMT samples. The phase structures are analyzed by General Structure Analysis System (GSAS) Rietveld refinements for 0.8BT-0.2BMT with various amount of Nb_2O_5, as shown in Figure 2. The main phase is detected as $BaTiO_3$ (P4mm, ICSD No. 086286). The lattice parameters and reliability factors are listed in Table 1. All the lattice parameters are obtained with high reliability as $R_{wp} < 10\%$, $R_p < 8\%$. The lattice parameters calculated from the Rietveld refinements increase continuously with the increase of Nb_2O_5 content. This indicated the larger ionic radius substitution that occurred according to Bragg's law. In other words, Nb^{5+} mainly enters the Ti-sites as a donor because the Nb^{5+} (0.64 Å) is a considerably larger radius than that of Ti^{4+} (0.605 Å) in six-fold coordination [17]. Meanwhile, Nb substitution on Ti site in the $BaTiO_3$ lattice will leave the excess Ti out of the grains, which is responsible for secondary phase formation at the grain boundary.

Table 1. Lattice parameters from Rietveld refinement for the samples.

Samples	Lattice Parameters			Reliability Factors		
	a (Å)	c (Å)	V (Å^3)	R_{wp}	R_p	χ^2
+0.0 mol% Nb_2O_5	4.0096	4.0131	64.5182	0.0786	0.0598	1.678
+1.0 mol% Nb_2O_5	4.0112	4.0140	64.5842	0.0873	0.0651	2.187
+2.0 mol% Nb_2O_5	4.0131	4.0165	64.6856	0.0780	0.0579	1.555
+3.0 mol% Nb_2O_5	4.0150	4.0179	64.7695	0.0847	0.0621	1.943

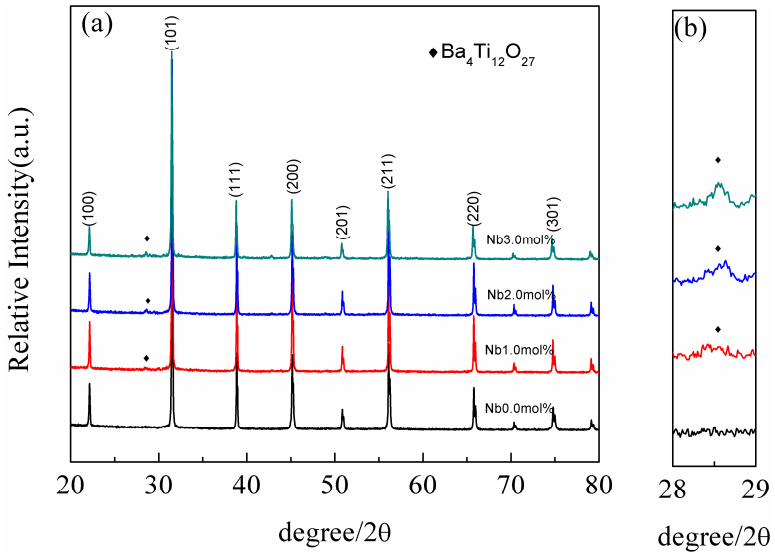

Figure 1. (**a**) The XRD patterns of well-sintered Nb_2O_5 doped 0.8BT-0.2BMT ceramic disks; (**b**) the XRD patterns in the region between 28 and 29 degree.

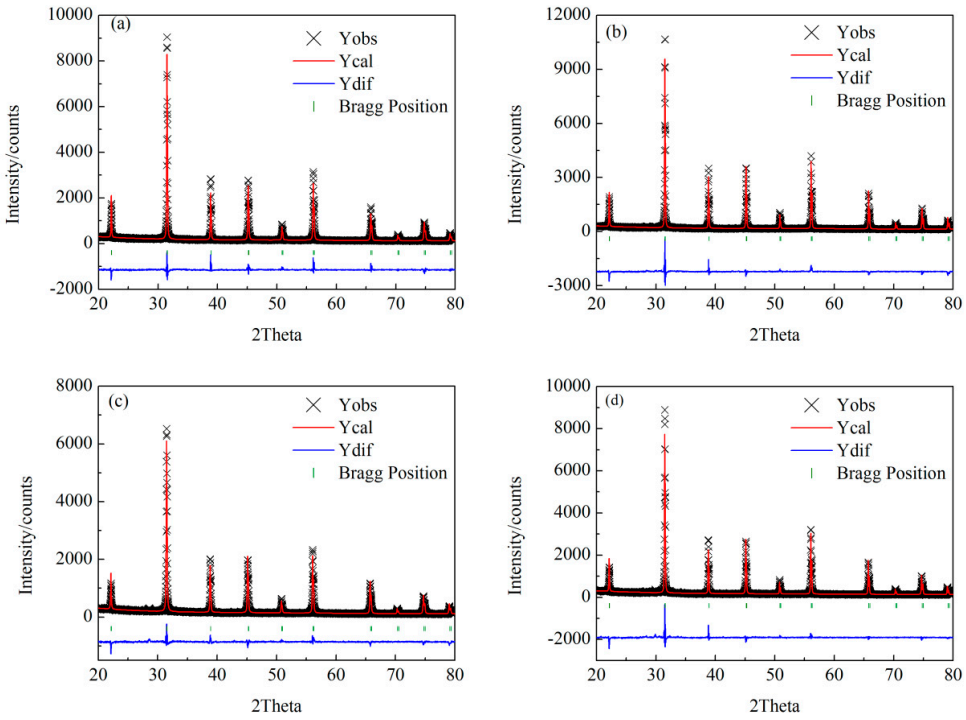

Figure 2. XRD profiles for the Rietveld refinement resultsfor 0.8BT-0.2BMTwith various amount of Nb_2O_5: (**a**) 0.0 mol%; (**b**) 1.0 mol%; (**c**) 2.0 mol%; (**d**) 3.0 mol%.

Figure 3 shows the microstructure of various amount of Nb_2O_5 doped 0.8BT-0.2BMT ceramics. It is observed that all the Nb-doped 0.8-0.2BZT ceramics are in high densification with homogeneous grain size being on the order of several micrometers. There is a small change of the grain size as the Nb_2O_5 content increases, where the average grain size is about 1.5 μm. Some stick grains, pointed by arrows in the Nb_2O_5 doped samples, are considered as secondary phase ($Ba_4Ti_{12}O_{27}$). This result is highly consistent with XRD analysis.

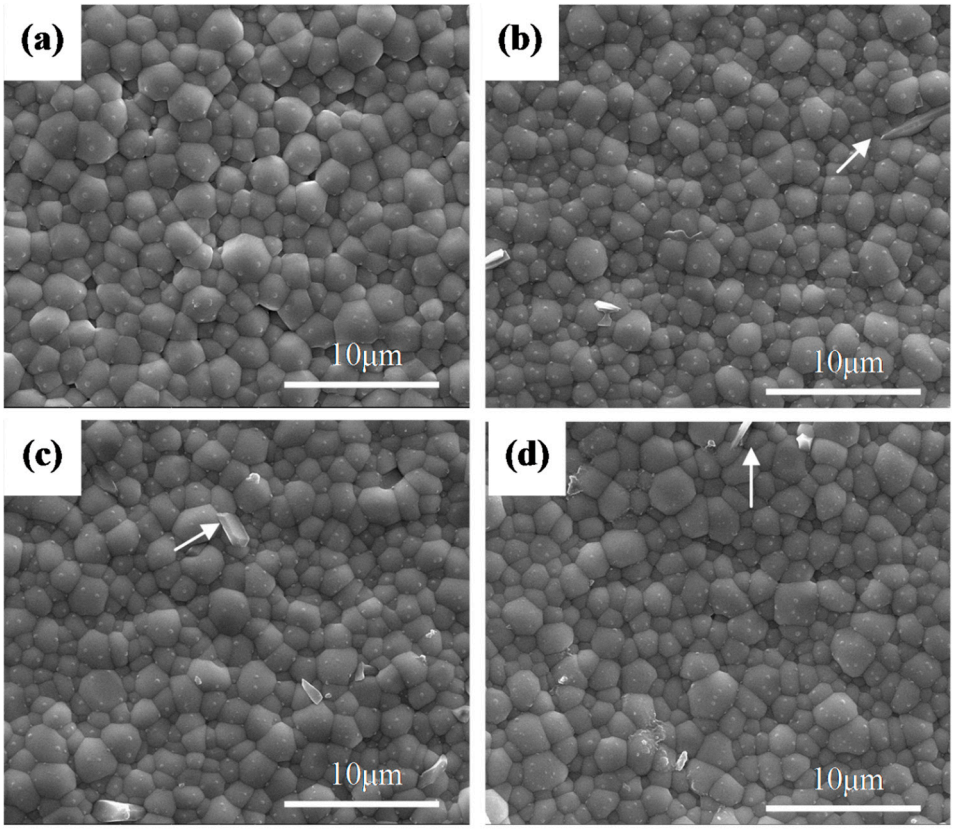

Figure 3. The microstructure of various amount of Nb_2O_5 doped 0.8BT-0.2BMT ceramics: (**a**) 0.0 mol%; (**b**) 1.0 mol%; (**c**) 2.0 mol %; (**d**) 3.0 mol%.

Main dielectric and electrical properties at room temperature of the samples are listed in Table 2. As we can see, dielectric constant at 25 °C decreased with increasing Nb_2O_5 content. In the Nb_2O_5 modified BT-BMT system, the Nb^{5+} will diffuse into the crystal lattice to form the chemically inhomogeneous structure ('core-shell'). The dielectric characteristics of the barium titanate-based core-shell grain structure were a superposition of the ferroelectric grain core, paraelectric grain shell [18]. With further addition of Nb_2O_5 dopants, the volume fractions of the shell region increased, leading to the decrease of the dielectric constant.

Table 2. Dielectric and electrical properties of the samples at room temperature.

Sample	ε_r	tan δ	$\Delta C/C_{25\,^\circ C} < \pm 15\%$	Resistivity (Ω·cm)	Density (g/cm^3)
+0.0 mol% Nb_2O_5	1683	5.0%	-	1.0×10^{13}	6.214
+1.0 mol% Nb_2O_5	1247	1.5%	−26~197 °C	6.4×10^{11}	6.219
+2.0 mol% Nb_2O_5	925	0.7%	−40~200 °C	5.9×10^{12}	6.148
+3.0 mol% Nb_2O_5	764	0.5%	−55~200 °C	1.3×10^{13}	6.159

When a small amount of Nb_2O_5 is doped into the BT matrix, electronic compensation regime appears [19–21].

$$Nb_2O_5 \rightarrow 2Nb_{Ti}^{\bullet} + 2TiO_2 + O_0 + 2e' \quad (1)$$

The insulation resistivity of the sample with 0.1 mol% Nb_2O_5 dopants decreased for the electronic compensation. With the increasing of Nb_2O_5 concentration, the electronic compensation changes into Ti vacancy compensation.

$$2Nb_2O_5 \rightarrow 4Nb_{Ti}^{\bullet} + 5TiO_2 + V_{Ti}^{''''} \quad (2)$$

The mechanism is mainly involved with the compensation of Ti vacancies so that the samples with 3.0 mol% Nb_2O_5 can become highly insulating as shown in Table 2 [22].

Figure 4 demonstrates the temperature dependence of dielectric constant and dielectric loss for 0.8BT-0.2BMT with various amount of Nb_2O_5. Double dielectric peaks are observed: one at around 0 °C and a second, smaller, peak at about 130 °C. The curves are flattened by the Nb_2O_5 dopants at the cost of deteriorating dielectric constant. However, when the doped level is above 2.0 mol%, it is difficult to detect the higher permittivity peak. Loss tangent data at room temperature are lower than 5%, and exhibit a decrease with increasing Nb_2O_5 content. Dielectric loss at low temperature is rather high and decreases monotonously with the increasing temperature.

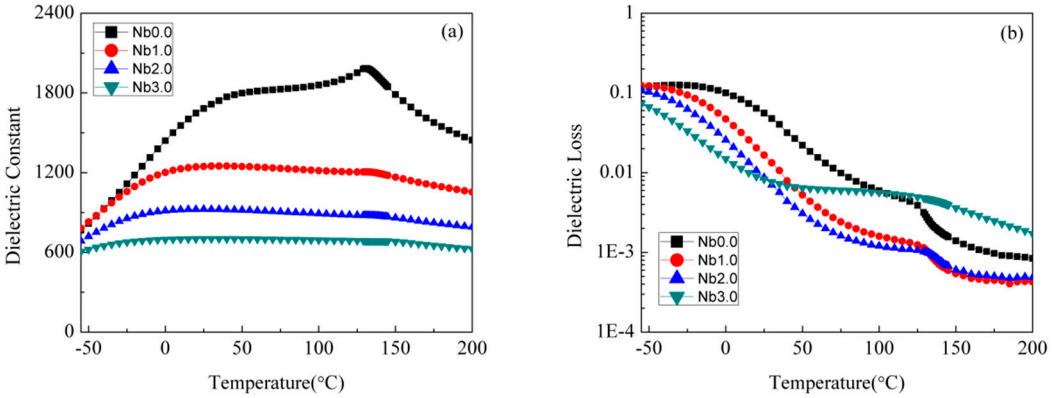

Figure 4. Temperature dependence of (**a**) dielectric constantand (**b**) dielectric loss for 0.8BT-0.2BMT with various amount of Nb_2O_5.

Temperature dependence of capacitance variation rate based on $C_{25\,^{\circ}C}$ for 0.8BT-0.2BMT with various amount of Nb_2O_5 is shown in Figure 5. It can be seen that the temperature-capacitance characteristics have a remarkable improvement with the incorporation of Nb_2O_5, especially at the cold end. At the hot end, the permittivity peak is suppressed with the increase of Nb_2O_5 dopants. The 3.0 mol% Nb_2O_5-doped 0.8BT-0.2BMT ceramic sample is found to satisfy the EIA X9R specification with a permittivity of 764 and dielectric loss of 0.5%. The existence of the double dielectric anomalies over the studied temperature range, which is the characteristic phenomenon of 'core–shell' structure in BT ceramics, is beneficial to improving the temperature stability of the dielectric properties [20]. The Nb^{5+} will diffuse into the crystal lattice to form the chemically inhomogeneous structure, where the core is pure BT, while the Nb ion mainly concentrated in the shell region. In the ceramics with 'core–shell' structure, the double peaks in the temperature dependence of dielectric constant curve can usually be obtained [14]. In the Nb_2O_5 modified 0.8BT-0.2BMT system, the dopant oxides tend to accumulate at the grain boundary and diffuse simultaneously into BT grain. Nevertheless, the diffusion of Bi ions was weakened due to the slow diffusion of Nb^{5+} during the sintering process. Thus Bi_2O_3, MgO, and TiO_2 mainly stayed in the shell region which should be responsible for the lower dielectric peak at ~0 °C, while pure BT at cores is attributable to the dielectric peak at ~130 °C, as shown in Figure 4.

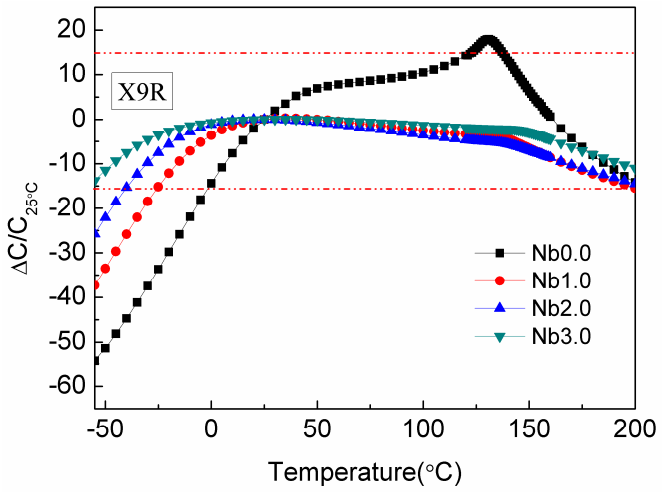

Figure 5. Temperature dependence of capacitance variation rate based on $C_{25\,^{\circ}C}$ for 0.8BT-0.2BMT with various amount of Nb_2O_5.

4. Conclusions

In this work, we investigated the effect of Nb_2O_5 doping on the dielectric properties of 0.8BT-0.2BMT ceramics. A small amount of $Ba_4Ti_{12}O_{27}$ secondary phase is observed when Nb_2O_5 doped into 0.8BT-0.2BMT system. The dielectric temperature stability is strongly affected by the Nb_2O_5 dopants. The 3.0 mol% Nb_2O_5-doped 0.8BT-0.2BMT ceramic sample satisfies the requirement of EIA X9R specification with a permittivity of 764. Moreover, it possesses low dielectric loss and high insulation resistance, which ensures the application of this material.

Acknowledgments: This work is supported by the Open Foundation of National Engineering Research Center of Electromagnetic Radiation Control Materials (ZYGX2016K003-5) and by National Natural Science Foundation of China (Grant No. 51402039)

Author Contributions: Bin Tang, Shuren Zhang and Feng Si conceived and designed the experiments; Feng Si performed the experiments; Bin Tang and Feng Si analyzed the data; Zixuan Fang contributed reagents/materials/analysis tools; Feng Si wrote the paper.

Conflicts of Interest: The authors declare no conflict of interest.

References

1. Johnson, R.W.; Evans, J.L.; Jacobsen, P. The changing automotive environment: High-temperature electronics. *IEEE Trans. Electron. Pack. Manuf.* **2004**, *27*, 164–176. [CrossRef]
2. Werner, M.R.; Fahrner, W.R. Review on materials, microsensors, systems, and devices for high-temperature and harsh-environment applications. *IEEE Trans. Ind. Electron.* **2001**, *48*, 249–257. [CrossRef]
3. Lee, W.H.; Su, C.Y. Improvement in the temperature stability of a $BaTiO_3$-Based multilayer ceramic capacitor by constrained sintering. *J. Am. Ceram. Soc.* **2007**, *90*, 3345–3348. [CrossRef]
4. Wang, S.F.; Dayton, G.O. Dielectric properties of fine-grained barium titanate based X7R materials. *J. Am. Ceram. Soc.* **1999**, *82*, 2677–2682. [CrossRef]
5. Sakayori, K.; Matsui, Y.; Abe, H. Curie-Temperature of Batio3. *Jpn. J. Appl. Phys.* **1995**, *34*, 5443–5445. [CrossRef]
6. Datta, K.; Thomas, P.A. Structural investigation of a novel perovskite-based lead-free ceramics: $xBiScO_3$-(1-x)$BaTiO_3$. *J. Appl. Phys.* **2010**, *107*, 043516. [CrossRef]
7. Raengthon, N.; Cann, D.P. Dielectric Relaxation in $BaTiO_3$-$Bi(Zn_{1/2}Ti_{1/2})O_3$ Ceramics. *J. Am. Ceram. Soc.* **2012**, *95*, 1604–1612. [CrossRef]
8. Liu, M.Y.; Hao, H.; Zhen, Y.C. Temperature stability of dielectric properties for $xBiAlO_3$-(1-x)$BaTiO_3$ ceramics. *J. Eur. Ceram. Soc.* **2015**, *35*, 2303–2311. [CrossRef]

9. Wang, Y.R.; Pu, Y.P.; Zheng, H.Y. Enhanced dielectric relaxation in (1-x)$BaTiO_3$-x$BiYO_3$ ceramics. *Mater. Lett.* **2016**, *181*, 358–361. [CrossRef]
10. Zeb, A.; Milne, S.J. High temperature dielectric ceramics: A review of temperature-stable high-permittivity perovskites. *J. Mater. Sci. Mater. Electron.* **2015**, *26*, 9243–9255. [CrossRef]
11. Ren, P.R.; Wang, X.; Fan, H.Q. Structure, relaxation behaviors and nonlinear dielectric properties of $BaTiO_3$-$Bi(Ti_{0.5}Mg_{0.5})O_3$ ceramics. *Ceram. Int.* **2015**, *41*, 7693–7697. [CrossRef]
12. Sun, Y.; Liu, H.X.; Hao, H. Structure Property Relationship in $BaTiO_3$-$Na_{0.5}Bi_{0.5}TiO_3$-Nb_2O_5-NiO X8R System. *J. Am. Ceram. Soc.* **2015**, *98*, 1574–1579. [CrossRef]
13. Hennings, D.F.K. Dielectric materials for sintering in reducing atmospheres. *J. Eur. Ceram. Soc.* **2001**, *21*, 1637–1642. [CrossRef]
14. Chazono, H.; Kishi, H. Sintering characteristics in the $BaTiO_3$-Nb_2O_5-Co_3O_4 ternary system: II, stability of so-called "core–shell" structure. *J. Am. Ceram. Soc.* **2000**, *83*, 101–106. [CrossRef]
15. Liu, X.A.; Cheng, S.G.; Randall, C.A. The core–shell structure in ultrafine X7R dielectric ceramics. *J. Korean Phys. Soc.* **1998**, *32*, S312–S315.
16. Toby, B.H. EXPGUI, a graphical user interface for GSAS. *J. Appl. Crystallogr.* **2001**, *34*, 210–213. [CrossRef]
17. Wang, T.; Jin, L.; Li, C.C. Relaxor Ferroelectric $BaTiO_3$-$Bi(Mg_{2/3}Nb_{1/3})O_3$ Ceramics for Energy Storage Application. *J. Am. Ceram. Soc.* **2015**, *98*, 559–566. [CrossRef]
18. Park, Y.; Kim, H.G. Dielectric temperature characteristics of cerium-modified barium titanate based ceramics with core–shell grain structure. *J. Am. Ceram. Soc.* **1997**, *80*, 106–112. [CrossRef]
19. Brzozowski, E.; Castro, M.S.; Foschini, C.R. Secondary phases in Nb-doped $BaTiO_3$ ceramics. *Ceram. Int.* **2002**, *28*, 773–777. [CrossRef]
20. Kowalski, K.; Ijjaali, M.; Bak, T. Electrical properties of Nb-doped $BaTiO_3$. *J. Phys. Chem. Solid.* **2001**, *62*, 543–551. [CrossRef]
21. Li, W.; Qi, J.Q.; Wang, Y.L. Doping behaviors of Nb_2O_5 and Co_2O_3 in temperature stable $BaTiO_3$-based ceramics. *Mater. Lett.* **2002**, *57*, 1–5. [CrossRef]
22. Smyth, D.M. The defect chemistry of donor-doped $BaTiO_3$: A rebuttal. *J. Electroceram.* **2002**, *9*, 179–186. [CrossRef]